Int. Agrophysics, 1999, 13, 391-395

PRESSURIZED METHODS FOR GRADING THE VULNERABILITY OF PODS SPLITTING*

G. Szwed, J. Tys, W. Strobel

Institute of Agrophysics, Polish Academy of Sciences, Doświadczalna 4, P.O. Box 201, 20-290 Lublin 27, Poland

Accepted March 5, 1998

A b s t r a c t. Loss of seeds due to pod splitting at the time of ripening makes it necessary to search for the methods that would allow for the adequate grading of the vulnerability of a given variety. These methods should also be convenient instruments in the search for the optimal technology and harvest term. A method of testing air cramming at a suitable pressure for the release of the existing stress perpendicular to the raphe and leading to the pods splitting. The amount of pressure at which the raphes come apart is the measure of its vulnerability to splitting. Studies were carried out on the blue, white and yellow lupines. Differences in the measured values of the force necessary for the separation of the pod raphe in relation to the species and varieties of the lupines being examined were noted. The differences result from the composition of the raphes, the composition and thickness of the sklerenhym layers such as the geometry of the pod.

The series of tests was performed including: the geometry of the pods (length, width, thickness, thickness of the walls of the pod), the necessary force for the separation of the pod's raphe. The strength of the raphe was found in a range from 40.2 to 151.7 G/mm for pods of yellow lupines while in the cause of pods of blue lupines it ranged from 16.5 to 84.0 G/mm.

The results for the blue lupines were compared to the field studies on the splitting of pods as well as the shedding of seeds during three successive growing seasons. They showed the significant relations between these features.

K e y w o r d s: pod, lupine, cracking, shedding

INTRODUCTION

Pods drying at heir maturation affects stresses that cause raphes splitting and seed shedding. The phenomenon is a natural feature of primitive plants (wild ones) which ensures the plant survival and species expansion. New species introduced into the cultivation inherit the trait (to more or less extent) which leads to serious losses during harvest.

Laboratory studies on the lupine pod vulnerability to splitting that have been carried out in Institute of Agrophysics, PAS in Lublin, allowed to develop a method as well as to prepare a diagnostic device for the splitting vulnerability of pods from various lupine varieties.

The purpose of the research was to estimate the pod splitting vulnerability using a pressure method. The material presented here is the result of a three-year investigation carried out with the use of blue lupine pods from the experimental fields of The Plant Breeding Station in Uhnin. Laboratory studies were compared to field experiments that were conducted in the Station. They consisted in counting the cracked pods and windfallen grains during plants' maturation.

ESSENCE AND REASONS FOR POD SPLITTING

Analyzing the mechanical resistance of lupine fruit, its morphological and anatomical structure that conditions the vulnerability to pod splitting should be taken into account. The basic pod-half structural element is a layer of fiber tissue formed from a thickened, fiber-like cells that are arranged obliquely in relation to the fruit axis. In individual varieties, the layer has different

*Paper presented at 6 ICA

sizes, wall thickness and fiber direction [2,4,5]. Those factors as well as the structure of raphes joining the pod-halves determine the vulnerability of the particular varieties and species of lupine towards splitting. However, the main reasons for splitting and torsional motions of pod-halves are humidity changes due to the tissue higroscopicity. Specific fibrous structure of parchment layer of pod-half inner part (sclerenchyma) has the primary meaning in formation of the highest stresses during drying, as mentioned above [1,2]. Such a structure of the pod-half fibrous tissue causes the strongest changes that take place during drying in the perpendicular direction to its arrangement. Hence, the values and direction of torsional stresses depend on the inclination angle of the fiber in relation to the pod-half axis as well as the normal lines perpendicular to the fibrous layer (Fig. 1).

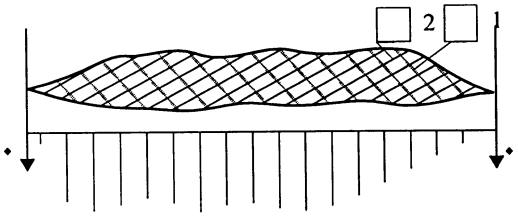

Fig. 1. Expected stress pattern in a pod: 1 - diretion of fibre orientation; 2 - normal lines (perpendicular) to the fibres.

The presented figure indicates that the highest torsional stresses occur in the middle of the pod-half where forces acting on a raphe joining both pod-halves are also the highest in this area. Thus, the beginning of splitting should be expected in a middle of the pod.

An additional important element connected to the mechanical resistance is a shape of the pod. Depending on the number and size of grains in the pod, pod-halves possess „swellings" reflecting the shape and the size of the grains inside.

Assuming that the P forces due to the contraction of the parchment layer fibers are the same for the pods with larger and smaller swellings, the former ones are more vulnerable to torsions (Fig. 2) because a smaller curvature radius causes increase of the arm (r_2) of the bending moment (Mg) in the plane in question (perpendicular to the direction of the fiber arrangement). A partial bending moment contributing to the pod-half twist is equal to:

$$Mg = Pr \tag{1}$$

where: P - the force depending on the drying extent of the parchment layer of fibers, r - the arm of the bending moment Mg.

Considering the system of action of forces as well as the arm length which these forces affect, it is clear that $r_2 > r_1$, thus Mg_2 for pod -half (Fig. 2b) is greater than Mg_1 for pod-half (Fig. 2a) because:

$$Mg_1 = Pr_1$$
$$Mg_2 = Pr_2. \tag{2}$$

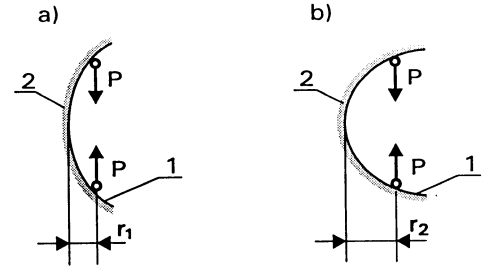

Fig. 2. Values of torsion moments twisting the pod that depend on its crowning: 1 - inner fibre layer; 2 - parenchyma layer; a - smaller radius of a pod curvature; b - bigger rading of a pod curvature.

Theoretical analyses made above prove that the values of stresses occurring on the pod's raphe and causing its splitting depend on the geometry and anatomical and the morphological structure of pod-halves. Drying process invokes stresses and their increase on the pod raphe till some critical values are achieved when the splitting stresses exceed the raphe cohesion forces and then pod-halves splitting as well as grain shedding take place.

It is interesting to find out where the splitting is going to begin: from the raphe concave side or the convex one ?

The lay-out of the pod intersection on the plane perpendicular to the inner fibers direction is presented in Fig. 3.

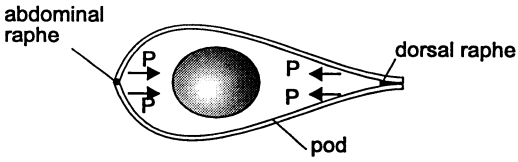

Fig. 3. Pod intersection in the discussed plane.

In the figure above, it is shown that the pod-half geometry in the neighbourhood of the raphes is different. Near the concave raphe on the intersection plane, pod-halves become almost a straight line adhering to each other with the minimum surface. Near the convex raphe, there is visible calix-like adhesion of pod-halves that are close to each other with their side surfaces which makes the contact surface greater than for the concave raphe. The bending moments Mg (on the intersection plane) due to the P forces also affect the stresses arisen in both raphes in different ways. The splitting stresses sr are formed on the concave raphe on its inner side, the compression stresses σ_s - on the outer side (Fig. 4a).

The bending moments affecting the pod -halves near the convex raphe press adhering pod-halves down to each other; thus affecting their splitting to a minimum extent. Thus, beginning of splitting can be expected on the ventral side of the pod. It is the place of natural pod opening.

Summing up, the pod-half geometry near raphes has a significant influence on the initiation of the pod splitting site.

METHODS AND STUDIES COURSE

A method developed in Institute is based on forcing the air with gradually increasing pressure into the pod interior till it splits [3]. The pressure value at splitting is the measure of the raphe durability.

The stand for the studies consisted with: reservoir in which there is pressured air complete with a pump, tensometrical converter connected to a computer and cut-off valve (Fig. 5).

During the air forcing, the pod is similar to a pressure vessel with a circular intersection for $g<D/20$, inside which there is a pressure p, where: g - pod-half wall thickness, D - pod diameter.

Here, we consider a planar stress state that occurs on the walls of the reservoirs loaded with liquid or gaseous pressure. The pressure directed towards both pod-halves tries to split them creating the maximum stresses on the pod raphe.

It can be proved considering the stress distribution on the separated squared pod-half part ABCD (Fig. 6). This element is under stretching towards the two perpendicular directions: axial

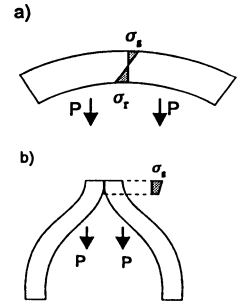

Fig. 4. Stresses distribution in raphes of lupine pods: a - concave raphe, b - convex raphe.

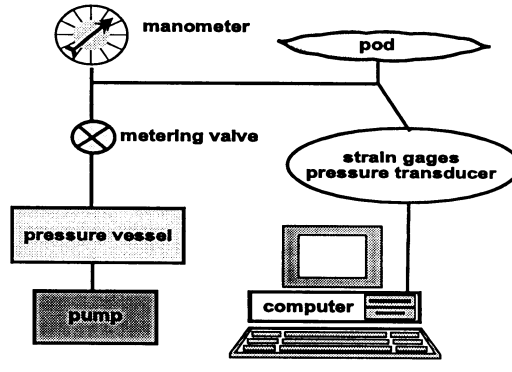

Fig. 5. Schematic diagram of the test stand.

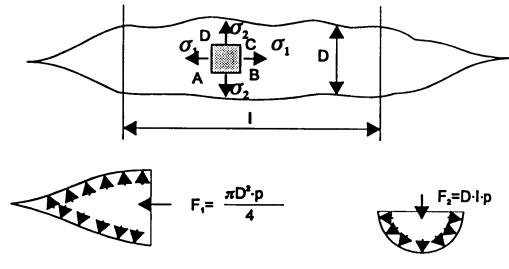

Fig. 6. Stress pattern in a pod D - diameter, l - length, F_1; F_2 - resultant force, p - pressure, σ_1 σ_2 - stress.

(along main axis of the pod) - stresses σ_1 as well as tangentially to the pod - stresses σ_2.

The force due to the pressure p acts on both ends of the pod in the axial direction and it is equal to the product of pod transverse intersection and pressure:

$$F_1 = \frac{\pi D^2}{4} p \ . \tag{3}$$

The force (F_1) is transferred by the pod transverse intersection that is a ring of thickness g and diameter D:

$$S_1 = \pi D g \ . \tag{4}$$

The axial stress in pod walls amounts to:

$$\sigma_1 = \frac{F_1}{S_1} = \frac{Dp}{4g} \ . \tag{5}$$

The circumferential stress σ_2 can be found as cutting the pod with a horizontal plane (along the raphes, for instance). Force due to the pressure is equal to the product of the pod-half surface projection onto the intersection plane and pressure:

$$F_2 = Dlp \ . \tag{6}$$

This force is transferred by a longitudinal intersection of the pod wall (raphe):

$$S_2 = 2lg. \tag{7}$$

The circumferential stress in question, equals to:

$$\sigma_2 = \frac{F_2}{S_2} = \frac{Dp}{2g} \ . \tag{8}$$

Comparing Eqs (5) and (8), it is clear that circumferential stresses in the pod (on the raphe) are twice as high as the axial ones. Thus, pod splitting takes place along the raphes.

STUDIES COURSE

The investigation process was preceded with the following operations:

1. Making the whole in the studied pod-half with a borer with the diameter close to the outer diameter of the syringe needle through which the air splitting the pod is introduced.

2. Placing the needle into the whole, and then sealing the joint needle-pod-half with a proper glue (plasticine) in order to prevent the forcing air leak from the pod during the pressure increase.

3. Connecting the pod and the needle to the measurement system (Fig. 5).

The gradual pressure increase in the pod and converter is invoked by valve opening. The pod raphe splitting causes the pressure decrease also in the converter (connected vessels) which is recorded on the computer monitor.

The pressure investigations were accompanied by some biometric measurements: length, width, thickness. The results of measurements were used for the elaboration of final results, among others, for computing the unitary splitting force per 1mm of the pod circumference [N/mm].

Studies were carried out in the three following years: 1994-1996 (Figs 7 and 8). Each sample consisted of 30 pods of blue lupine at pod-half humidity during measurement from 10.4 to 11.7%.

Figures present a graphical estimation of the study results. They show that there is a relation between pod splitting and seed shedding and the values of the unit forces splitting the pod and formed as a result of air pressure inside the pod. For all the investigated varieties, that relation is inversely proportional: the higher the shedding percentage, the lower the pressure (expressed in N/mm of the pod raphe circumference) required for surpassing the coherence forces of the pod raphe.

CONCLUSIONS

1. The results obtained point out to the fact that there is a relation between the values of forces splitting the raphe and results from the field studies (pod splitting and seed shedding). It is an inversely proportional relation: the lower the splitting force value, the greater the number of pods split. Such trends were observed in 1994 and 1995. The study results of 1996 are different because of the fact that high precipitations

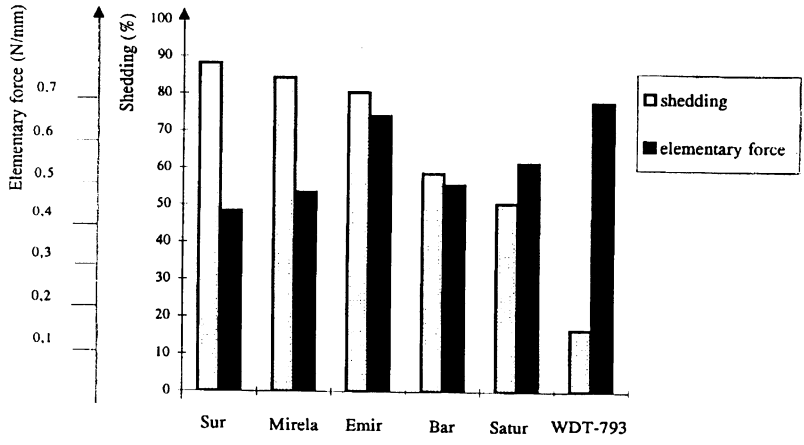

Fig. 7. Relation between grain shedding in the field depending on the value of the elementary force applied to achieve pod splitting of various narrow-leaved lupine (1995).

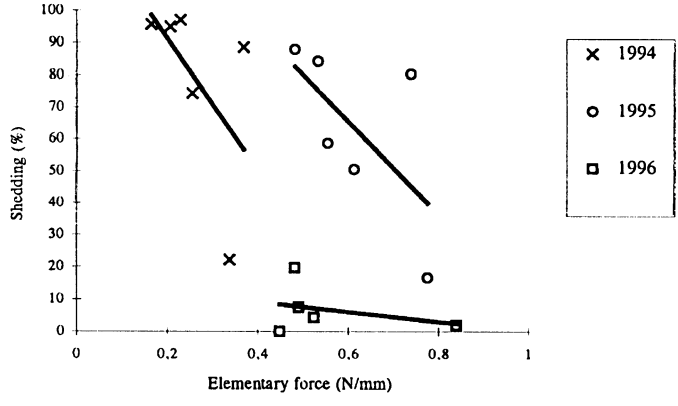

Fig. 8. Values of grains shedding on a field and elementary force applied for splitting of pods of various narrow-leaved lupine (1994, 1995, 1996).

caused pod infection of pods with fungus diseases.

2. The studied blue lupine fruits showed, differentiated inclination to splitting during the investigation period. Hence, there is the need for the estimation of variability in this feature in particular varieties taking into account weather conditions as well as the need to design simple and easy laboratory method for the prediction of vulnerability to seed shedding in the field conditions.

3. The pressurized method proposed here is the base for further investigations on the fruits of leguminous plant.

REFERENCES

1. **Jasińska Z., Kotecki A.:** Pulse Crops (in Polish). WN PWN 1993.
2. **Strasburger E.:** Botany (in Polish). PWRiL Warszawa, 1972.
3. **Szwed G., Falęcki A., Tys J.:** The method of pods crack resistance evaluation (in Polish). Lupin: scope of investigations and prospects of application. Polish Lupin Association and Institute of Bioorganic Chemistry, Polish Academy of Sciences, Poznań, 331-337, 1996.
4. **Tomaszewski Z.:** Breeding of yellow lupine with non-bursting and non-dropping pods (in Polish). Acta agrobotanica, 89-104, 1953.
5. **Tomaszewska Z.:** Introductory anatomical examination of lupine pods (in Polish). Acta agrobotanica, II, 151-177, 1954.

Int. Agrophysics, 1999, 13, 397-399

RELATIONSHIPS BETWEEN GLUTEN CONTENT AND GRINDING PROPERTIES OF WHEAT
(a short communication)*

F. Le Deschault de Monredon[1], *J. Laskowski*[2], *M.F. Devaux*[1]

[1]Institut National de la Recherche Agronomique, I.N.R.A., P.O. Box 71627, 44316 Nantes cedex 03, France
[2]Department of Machine Operation in Food Industry, University of Agriculture, Doświadczalna 44 20-236 Lublin, Poland

Accepted April 27, 1998

A b s t r a c t. In 14 wheat samples from mixed varieties, the wet gluten content was significantly correlated with grinding energy and particle size of flours. The particle size distributions were bimodal with a main mode between 570 and 690 μm and a second mode between 28 and 34 μm. The main mode was higher for samples with a high gluten content. Conversely, samples with a low gluten content exhibited a higher second mode. A grinding ability index calculated as the quotient of specific grinding energy to specific surface was highly correlated with the gluten content (r=0.90).

K e y w o r d s: wheat, gluten, hardness, particle size

INTRODUCTION

Gluten is the water-insoluble portion of cereals proteins and is a major functional component of wheat (*Triticum aestivum*) in bread processing. Gluten content depends on genetic and agronomic factors. Hard wheat varieties generally contain more gluten than soft wheat and are selected for that use. Bread flour is usualy made from hard wheat, largely because of its relatively high protein content and desirable quality. The actual hardness of wheat is in itself of some significance, as hard wheats yield flour of a granular character considered desirable in breadmaking [5]. In the present work the grinding properties of wheat and the particle size of flours were compared to the wet gluten content. The objective of the study was to investigate the interest of measuring physical properties for wheat stocking organisms.

MATERIAL AND METHODS

The wet gluten content was measured by washing technique and Arpin's method [4] for 14 samples from mixed varieties collected in Polish stocking organisms near Lublin.

All the samples were conditioned to 12% moisture content in a controlled atmosphere. This rate of moisture was chosen to preserve the samples.

Studies on the energy consumption of grinding processes were carried out on a laboratory hammermill (Culatti, Prolabo, France). The screen size was 1 mm. The energy required for grinding 2 g of kernels of each wheat was measured. The consumptions of monophase electric current with the frequency 100 Hz were recorded and analysed using a special computer programme [3]. Measurements were repeated 5 times.

The particles of flours were sized using a laser diffraction apparatus (Malvern Mastersizer, Malvern Instruments S.A., France) fitted with focal length lens of 1000 mm. A

*Paper presented at 6 ICA

water-suspended sample (2x3 g) was passed through the laser beam, which was diffracted as a function of particle size. The lens focused the laser light onto a 32-element, concentric, light sensitive ring photodiode detector. The radii of the rings were such that the size ranged between 4 and 2000 μm. The resulting distribution comprised 32 particle size classes, and their corresponding proportions of volume. The distributions were analysed by assesing the median diameter, d(v0.5) and the mode. The specific surface S (m^2g^{-1}), was calculated as :

$$S = 6/\rho\ D(3,2)$$

where ρ is the density 1.4, $D(3,2)$ is the surface equivalent mean diameter or Sauter diameter.

RESULTS

The gluten content and grinding properties of the 14 samples are described in Table 1.

The wet gluten content ranged from 18 to 33% and was 26.1 ± 4.1 in average.

The grinding energy which measured the resistance of kernels during grinding ranged from 108 to 148 J g^{-1} and was 126 ± 13 on average. The grinding energy was slightly correlated with the wet gluten content (r^2 = 0.42).

As already shown by several authors [1,2, 6], particle size distributions of ground wheat samples were bimodal (Fig. 1): the level of the main mode was 570-690 μm; the level of the other mode was 28-34 μm. The main mode was higher for high gluten content (Fig. 1a). The rate of the 28-34 μm mode was negatively correlated with the gluten content (r^2 = 0.66). Five samples, among the seven samples with a low gluten content, showed a small percentage of particles under 5 μm which were almost non existent for the other wheats (Fig. 1b). Calculated specific surface ranged from 0.054 to 0.122 $m^2\ g^{-1}$ and was 0.077 ± 0.022 in average.

A grinding ability index taking into account grinding kernel energy and flour particle size is proposed:

$$\text{grinding ability index} = \frac{\text{specific grinding energy (J g}^{-1})}{\text{specific surface (m}^2\text{g}^{-1})}\ (\text{J m}^{-2}).$$

The grinding ability index was highly correlated with the gluten content, r^2=0.82 (Fig. 2).

CONCLUSION

Measurements of particle size of flours by laser diffraction precisely discribed second mode of fine particles between 5 and 75 μm, higher for low gluten content. The grinding ability of mixed varieties of wheat in relation with the gluten content was shown taking into account energy and surface area at the same time.

Table 1. Gluten content and grinding properties

Wet gluten content (%)	Grinding energy (J g^{-1})	d(v0.5) (μm)	Specific surface (m^2g^{-1})	Small particles mode rate (%)
33.0	142	497	0.059	19.0
32.0	148	489	0.061	20.0
29.0	142	481	0.054	18.3
28.0	113	441	0.060	20.5
27.0	118	425	0.067	22.4
26.8	118	429	0.065	21.5
25.6	131	427	0.064	26.7
25.5	113	385	0.070	21.5
24.5	128	374	0.095	20.7
24.0	123	366	0.078	26.7
23.6	115	356	0.073	25.8
22.6	129	317	0.119	21.5
20.1	108	338	0.104	28.3
18.0	123	295	0.122	31.6

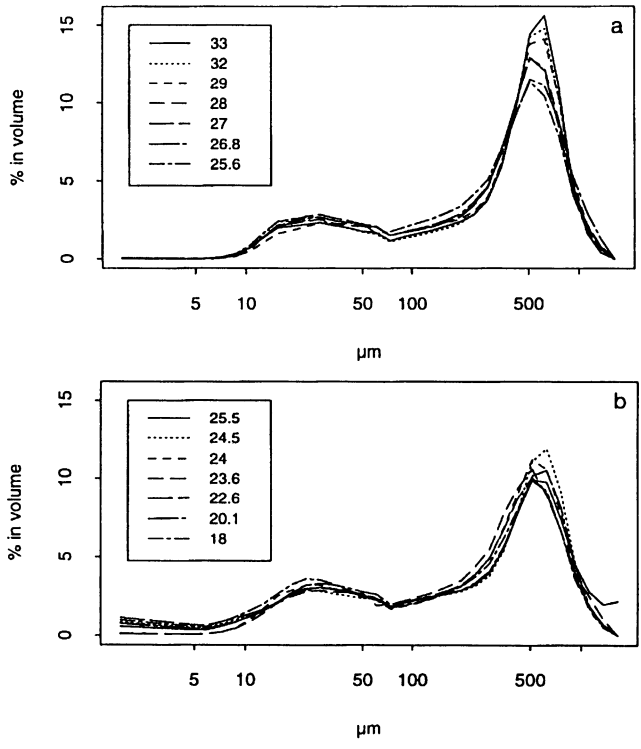

Fig. 1. High (a) and low (b) gluten content particle size.

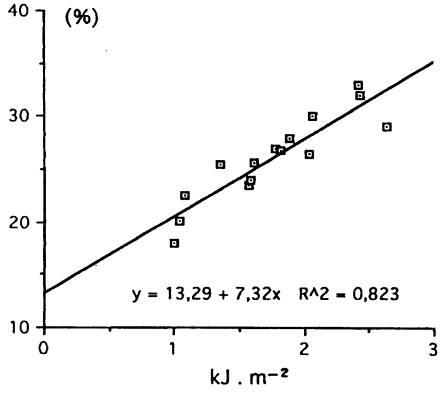

Fig. 2. Correlation between gluten content and grinding ability index.

REFERENCES

1. **Devaux M.F., Le Deschault de Monredon F., Guibert D., Navales B., Abecassis J.:** Particle size distribution of break, sizing and middlings flours by laser diffraction for nine French wheat varieties differing in kernel hardness. J. Sci. Food Agric., 78, 2, 237-244, 1998.
2. **Hareland G.A.:** Evaluation of flour particle size distribution by laser diffraction, sieve analysis and near-infrared reflectance spectroscopy. J. Cereal Sci., 21, 183-190, 1994.
3. **Laskowski J., Łysiak G.:** Experimental set-up for granulation process desting of biological raw-materials (in Polish). Postępy Techniki Przetwórstwa Spożywczego, 6, 1/2, 55-58, 1997.
4. **Lecoq R.:** Manuel d'analyses alimentaires et d'expertises usuelles. Editions Doin, Paris, 961-964, 1965.
5. **Pomeranz Y.:** Wheat, Chemistry and Technology. Am. Assoc. Cereal Chem Inc., St. Paul, Minnesota, USA, 24, 1971.
6. **Willm Cl.:** Comportement en mouture de 9 variétés de blé tendre. Influence de la dureté sur la granulométrie des farines. Ind. Céréales, 10, 2-9, 1995.